V-Shaped dc Potential Structure Caused by Current-Driven Electrostatic Ion-Cyclotron Instability

Seiji Ishiguro
Department of Electronic Engineering, Tohoku University, Sendai 980-77, Japan

Tetsuya Sato, Hisanori Takamaru, and The Complexity Simulation Group*
Theory and Computer Simulation Center, National Institute for Fusion Science, Nagoya 464-01, Japan
(Received 20 February 1997)

It is first demonstrated that a V-shaped dc potential structure is created by a current-driven electrostatic ion-cyclotron instability by means of an open two-dimensional particle simulation model. A positive dc potential difference along magnetic field lines is generated by anomalous resistivity caused by the ion-cyclotron instability. In the direction across the magnetic field lines, the dc potential rises from the high-current region to the low-current region. [S0031-9007(97)03467-4]

PACS numbers: 52.35.Qz, 52.65.Rr, 94.20.Qq, 94.20.Ss

Formation of electric field along magnetic field lines is as yet a puzzling and challenging problem for generating accelerated charged particles in a space plasma [1]. In particular, many space observations support the theory that auroral electrons are accelerated by a parallel electric field above the ionosphere [2–4]. Current-driven kinetic instabilities such as ion acoustic and electrostatic ion-cyclotron instabilities have been paid much attention as such candidates. It is well known that double layers are created by an ion acoustic instability for a relatively high electron stream [5–7]. On the other hand, analysis says that electrostatic ion-cyclotron waves become unstable for a smaller electron stream in an isothermal plasma [8,9] and in fact that are frequently observed by satellite observations. Furthermore, it is reported that a V-shaped potential structure and electrostatic ion cyclotron wave are simultaneously present above the auroral ionosphere [10]. In the past Swift [11] proposed an auroral electron acceleration model based on a oblique electrostatic shock caused by a current-driven electrostatic ion-cyclotron instability. However, the steady state theory cannot answer the question how shock is created. Although many laboratory experiments [12,13] and numerical simulations [14,15] concerned with a V-shaped potential structure or an ion-cyclotron instability have been performed, noone succeeded in demonstrating that current-driven electrostatic ion-cyclotron instability creates a V-shaped potential structure.

With these situations in mind, we investigate development of a current-driven electrostatic ion-cyclotron instability and resulting dc potential structure with special attention on two-dimensional structure by means of a sophisticated particle simulation model.

In our previous particle simulation [16], we observed a clear wave front pattern accompanied by the ion-cyclotron instability. In that simulation we used a periodic boundary condition for both particles and fields, namely, particles going out one boundary periodically enter the system from the other boundary. Because of no supply of fresh streaming particles the growth of the wave amplitude saturates at a low level and no observable dc potential structure is created. In the auroral field line region, however, the origin of the streaming electrons along the field lines is supposed to be in the plasma sheet. This means that the field-aligned electron stream, or field-aligned current, is continuously supplied by fresh magnetospheric electrons. Therefore, the periodic boundary condition is not appropriate for both particles and fields. In order to remove the periodic boundary condition and to make a more realistic situation, we have developed a two-and-a-half dimensional open boundary simulation code adopting the method developed by Takamaru *et al.* [7,17] for a one-dimensional simulation.

We have developed a two-and-a-half dimensional electrostatic open boundary particle simulation model where fresh particles are injected from the boundaries at each time step avoiding unphysical accumulation of charged particles in front of the boundaries. A schematic view of the simulation model is presented in Fig. 1. Uniform external magnetic field is pointing into the positive x direction. A

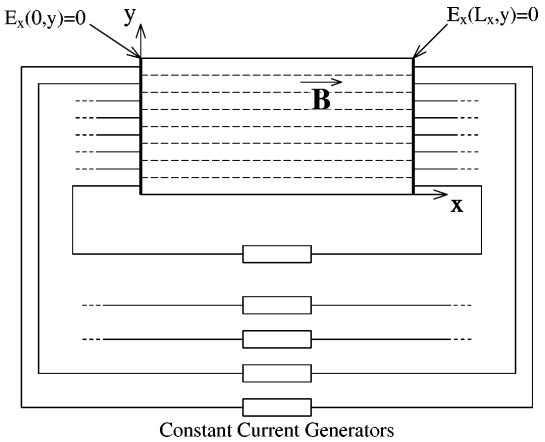

FIG. 1. Open boundary simulation system connected to constant current generators.

periodic boundary condition is applied in the y direction, whereas the left and right boundaries are open. The system is divided in segments in the y direction where each segment is assumed to be connected to an external constant current generator, respectively. The number of particles injected from the open boundaries in the x direction is specified in such a way that the electric current is kept constant at the boundaries of each segment at each time step. The velocity distribution of injected particles is specified so as to be consistent with the initial particle velocity distribution. This procedure is applied for electrons. For ions, however, the reflection boundary condition is applied. This is because we assume a shifted Maxwellian electron and a nonshifted Maxwellian ion.

The ion motion is followed in (v_x, v_y, v_z) velocity space and (x, y) real space to track the ion cyclotron motion, whereas we adopt the drift kinetic approximation for electrons and the electron motion is traced only along the magnetic field lines. This is because the electric field has only x and y components, so particle $\mathbf{E} \times \mathbf{B}$ drift motion is pointing into the z direction which has no meaning in our configuration.

Simulation parameters used in this paper are as follows: The system sizes are $L_x = 512\lambda_{\mathrm{De}}$ and $L_y = 128\lambda_{\mathrm{De}}$ and the grid number is 512×128, where λ_{De} is the Debye length. The system is assumed to be divided into 16 segments in the y direction, and thus the width of each segment is $8\lambda_{\mathrm{De}}$. The number of ions and electrons is 67 108 864, respectively, and, thus, 1024 particles per unit grid cell are used. The ion to electron mass ratio is 400 and the temperature ratio is $1/2$. The electron cyclotron frequency $\omega_{\mathrm{ce}} = 5\omega_{\mathrm{pe}}$ and the ion cyclotron frequency is $\omega_{\mathrm{ci}} = 0.0125\omega_{\mathrm{pe}}$, where ω_{pe} is the electron plasma frequency. The electron velocity distribution is a shifted Maxwellian with drifting into the x direction, and the drift velocity is given by $v_{\mathrm{de}}(y) = [0.6 - 0.2\cos(2\pi y/L_y)]v_{\mathrm{te}}$. Here, $v_{\mathrm{te}}[= (T_e/m_e)^{1/2}]$ is the electron thermal velocity, T_e and m_e are, respectively, the electron temperature (energy unit) and the electron mass. The time step width $\omega_{\mathrm{pe}}\Delta t$ is 0.2.

First of all, we show the growth of ion-cyclotron instability. Figure 2 shows time evolution of the magnitude of the ion density fluctuation [2(a)] and the frequency spectrum [2(b)] for the mode with $k_\perp \rho_i = 0.825$ and $k_\parallel \rho_i = 0.103$, where we use $\cos k_x x \exp ik_y y$ transform to obtain spatial spectrum. This is the typical unstable mode for the electrostatic ion cyclotron wave for our choice of simulation parameters. It should be noted that the amplitude of the ion density fluctuation continuously increases for a long time, whereas in the previous simulation [16] with the periodic model (the same parameters) the growth saturates at a lower level around $\omega_{\mathrm{pe}} t \simeq 4000$. This indicates that the injection of fresh drifting electrons from the boundaries much more activates the instability development. The peaks of the frequency are around $\omega \simeq \pm 1.4\omega_{\mathrm{ci}}$, indicating that the mode corresponds to the ion cyclotron wave, which has a phase velocity $\omega/k_\parallel \simeq 0.5v_{\mathrm{te}}$ and $\omega/k_\perp \simeq 0.06v_{\mathrm{te}}$, and thus propagates ± 83 degrees with respect to the magnetic field with speed $\omega/|k| \simeq 0.06v_{\mathrm{te}}$.

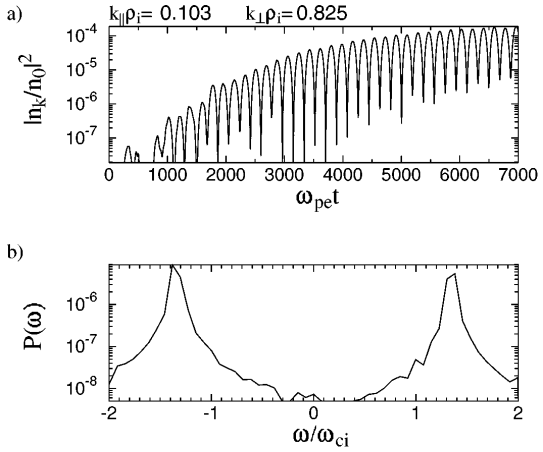

FIG. 2. Time history of ion density fluctuation (a) and frequency spectrum (b) with $k_\parallel \rho_i = 0.103$ and $k_\perp \rho_i = 0.825$.

We shall show a long time evolution of the ion density profile, which is averaged over the three times of the electron plasma period $3 \times 2\pi/\omega_{\mathrm{pe}}$ in Fig. 3. At $\omega_{\mathrm{pe}} t = 500$, one can see only small scale smeared fluctuations in the whole system. It is important to note that no

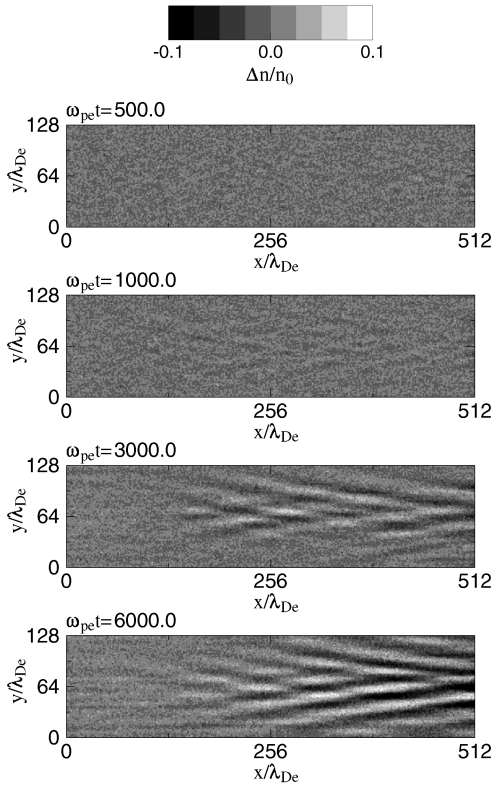

FIG. 3. Gray scale plots of the ion density fluctuation at $\omega_{\mathrm{pe}} t = 500$, 1000, 3000, and 6000.

sheathlike or any artificial noises appear near the upstream and downstream boundaries, although fresh electrons are injected from the boundaries. A V-shaped stripe pattern appearing at $\omega_{pe}t = 1000$ in the region with $x/\lambda_{De} \gtrsim 150$ and $30 \lesssim y/\lambda_{De} \lesssim 100$ grows with time and becomes clear at $\omega_{pe}t = 3000$. At $\omega_{pe}t = 6000$, a V-shaped wave front pattern is well developed for $x/\lambda_{De} \gtrsim 200$. The angle between the wave front and the magnetic field lines is $\pm 7°$, namely, $|k_y/k_x| \simeq 0.12$. The amplitude is larger in the downstream region than in the upstream region.

Figure 4 shows the gray scale contour plots of the potential profile at $\omega_{pe}t = 6000$. A clear V-shaped wave front pattern is seen around $x/\lambda_{De} \sim 380$ and $y/\lambda_{De} \sim 70$. The angle between the equipotential lines and magnetic field lines is $\pm 7°$, which is the same as for the ion density profile.

In order to see the time variation of the ion density profile in a short time interval, we plot the ion density profiles at 5900, 6000, and 6100 in Fig. 5. Careful examination of three profiles concludes that the wave front propagates with angle $\pm 83°$ with respect to the magnetic field. The wave length is roughly $20\lambda_{De}$ and the speed of propagation is roughly $0.06v_{te}$. These indicate that the mode with $k_\parallel \rho_i \simeq 0.1$ and $k_\perp \rho_i \simeq 0.8$ is dominant. It is to be noted that the wave which propagates with angle $+83°$ with respect to the magnetic field has a larger amplitude than the wave which propagates with angle $-83°$ in the upper half plane and vice versa in the lower half plane. Thus, we can see a V-shaped wave front pattern which consists of the waves propagating from the high-stream region (around $y/\lambda_{De} \simeq 64$) to the low-stream region (around $y/\lambda_{De} \simeq 0$ and 128).

Finally, we shall see the dc potential profile. Figure 6 shows that the gray scale contour plot of potential profile together with the potential profiles along the magnetic field lines at $y/\lambda_{De} = 64$ and across the magnetic field lines at $x/\lambda_{De} = 320$, 370, and 430. These are averaged over the period of oscillation of the electrostatic ion cyclotron wave. The potential gradually rises up from $x/\lambda_{De} \simeq 300$ to the downstream boundary along the magnetic field lines. The total potential difference reaches about $e\Delta\phi/T_e \simeq 0.02$.

The anomalous resistivity can be calculated from the relation $\eta = eE/n_0e^2v_{de} = e(\Delta\phi/l)\phi/n_0e^2v_{de}$. Using the above results with $e\Delta\phi/T_e \simeq 0.02$, $l = 200\lambda_{De}$, $v_{de} = 0.8v_{te}$, one can get $\eta/\eta_0 \simeq 1.2 \times 10^{-4}$, where $\eta_0 = 4\pi/\omega_{pe}$. In the y direction the potential profile has a small well. Though not so clearly structured, one can certainly recognize a V-shaped dc potential structure in the downstream region.

The linear kinetic analysis for spatial uniform electron stream with $v_{de} = 0.8v_{te}$ predicts that the modes with $0.08 \lesssim k_\parallel \rho_i \lesssim 0.2$ and $0.4 \lesssim k_\perp \rho_i \lesssim 1.5$ are unstable. Furthermore, the mode presented in Fig. 2 is in the large growth rate region and has a real frequency close to the observed one. The result shown in Fig. 5 also indicates that it is a dominant mode.

In the previous periodic boundary simulation [16], we have observed a significant modification of the electron velocity distribution and the decay of electron current as the amplitude grows due to the instability. On the contrary, the modification of the electron velocity distribution is small and the current is kept constant in the present open simulation since fresh electrons are supplied from the boundaries. Hence the amplitude of the ion cyclotron wave grows continuously beyond the level of saturation of the previous periodic particle simulation.

The ion cyclotron wave is excited in the upstream region and develops as it propagates from the upstream region to the downstream region with $\pm 83°$ with respect to the magnetic field. It grows significantly when it crosses the high electron-stream region; thus, it has a large amplitude when it propagates from the high electron-stream region to the low region. Hence a V-shaped wave front pattern arises.

It is interesting to observed that a V-shaped dc potential structure is created by the electrostatic ion-cyclotron instability. The dc potential gradually grows from the center

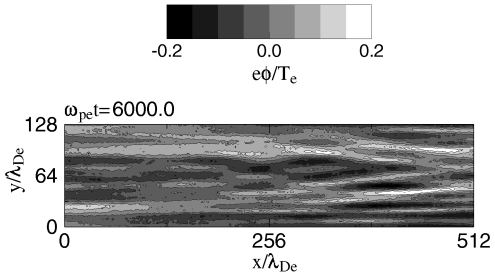

FIG. 4. Gray scale contour plot of the potential profile at $\omega_{pe}t = 6000$.

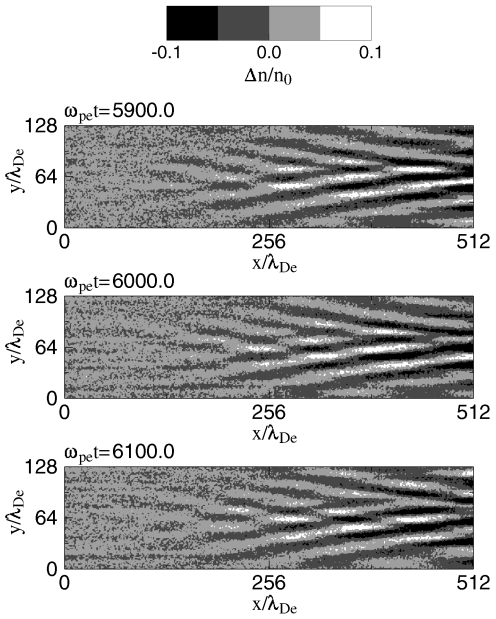

FIG. 5. Gray scale plots of the ion density fluctuation at $\omega_{pe}t = 5900$, 6000, and 6100.

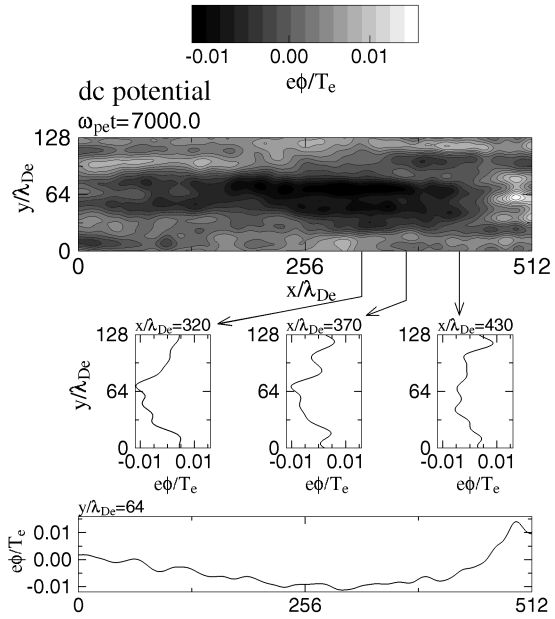

FIG. 6. Gray scale contour plot of the dc potential profile together with the x direction profile at $y/\lambda_{\mathrm{De}} = 64$ and the y direction profiles at $x/\lambda_{\mathrm{De}} = 320$, 370, and 430 at $\omega_{\mathrm{pe}}t = 7000$.

of the system to the downstream region. This dc potential difference along the magnetic field lines is supposed to be created by the anomalous resistivity caused by the ion cyclotron waves. The potential difference is larger in the high electron-stream region than in the low electron-stream region. The anomalous resistivity estimated from the created potential difference is much larger than the value obtained from the initial value periodic simulation.

We have observed a potential well across the magnetic field lines. This may be caused by the ion transport from the high-stream region to the low-stream region or the difference of ion perpendicular heating across the magnetic field lines.

The growth of the amplitude of ion cyclotron wave stops neither temporally nor spatially within the limit of the present simulation run. Thus it is likely that a larger potential difference may be created for a larger and longer simulation system. If we assume that the potential difference is proportional to the system length, one can get several kV potential differences for $T_e = 1$ eV, $n_e = 10^2$ cm^{-2}, and several thousand kilometers anomalous resistivity region [18], which is consistent with the auroral electron acceleration.

In conclusion we have succeeded in completing for the first time a two-dimensional particle simulation which demonstrates that the V-shaped dc potential structure is created by the current-driven electrostatic ion-cyclotron instability.

One of the authors (S. I.) thanks Professor Noriyoshi Sato for his encouragement. The computations were performed at the Advanced Computing System for Complexity Simulation at the National Institute for Fusion Science.

*K. Watanabe, R. Horiuchi, T. Hayashi, Y. Todo, T.-H. Watanabe, and A. Kageyama.

[1] C.-G. Fälthammar, Rev. Geophys. Space Phys. **15**, 457 (1977).
[2] L. A. Frank and K. L. Ackerson, J. Geophys. Res. **76**, 3612 (1971).
[3] D. Evans, J. Geophys. Res. **79**, 2853 (1974).
[4] R. L. Arnoldy, P. B. Lewis, and P. O. Issacson, J. Geophys. Res. **79**, 4208 (1974).
[5] T. Sato and H. Okuda, Phys. Rev. Lett. **44**, 740 (1980); J. Geophys. Res. **86**, 3357 (1981).
[6] C. Barnes, M. K. Hudson, and W. Lotko, Phys. Fluids **28**, 1055 (1985).
[7] T. Sato, H. Takamaru, and The Complexity Simulation Group, Phys. Plasmas **2**, 3609 (1995).
[8] W. E. Drummond and M. N. Rosenbluth, Phys. Fluids **5**, 1507 (1962).
[9] J. M. Kindel and C. F. Kennel, J. Geophys. Res. **76**, 3055 (1971).
[10] F. S. Mozer, C. W. Carlson, M. K. Hudson, R. B. Torbert, B. Parady, J. Yatteau, and M. C. Kelley, Phys. Rev. Lett. **38**, 292 (1977).
[11] D. W. Swift, J. Geophys. Res. **84**, 6427 (1979).
[12] M. J. Alport, S. L. Cartier, and R. L. Merlino, J. Geophys. Res. **91**, 1599 (1986).
[13] N. Sato, M. Nakamura, and R. Hatakeyama, Phys. Rev. Lett. **57**, 1227 (1986).
[14] J. S. Wagner, T. Tajima, J. R. Kan, J. N. Leboeuf, S.-I. Akasofu, and J. M. Dawson, Phys. Rev. Lett. **45**, 803 (1980).
[15] H. Okuda, C. Z. Chen, and W. W. Lee, Phys. Fluids **24**, 1060 (1981).
[16] S. Ishiguro, T. Sato, H. Takamaru, K. Watanabe, and The Complexity Simulation Group, "Formation of Wave-Front Pattern Accompanied by Current-Driven Electrostatic Ion-Cyclotron Instabilities" (to be published).
[17] H. Takamaru, T. Sato, R. Horiuchi, K. Watanabe, and The Complexity Simulation Group, "A self-Consistent Open Boundary Model for Particle Simulation in Plasmas" (to be published).
[18] M. K. Hudson, R. L. Lysak, and F. S. Mozer, Geophys. Res. Lett. **5**, 143 (1978).